

Photochemical Hydrogen Desorption from H-Terminated Silicon(111) by VUV Photons

A. Pusel, U. Wetterauer, and P. Hess

Institute of Physical Chemistry, University of Heidelberg, Im Neuenheimer Feld 253, 69120 Heidelberg, Germany

(Received 4 December 1997)

The 7.9 eV photons of a F₂ laser induced photochemical desorption of molecular hydrogen from Si(111)-(1 × 1):H surfaces with a cross section of $(1.2 \pm 0.8) \times 10^{-20}$ cm². The time-of-flight detection of desorbing species and numerical calculations of surface heating clearly allowed photochemical F₂-laser (7.9 eV) desorption and photothermal XeCl-laser (4.0 eV) desorption to be distinguished. Molecular dynamics simulations indicate the appearance of atomic and molecular hydrogen. The efficiency of photodissociation and desorption is higher than for the electron-stimulated process. [S0031-9007(98)06646-0]

PACS numbers: 82.65.-i, 82.20.Fd, 82.50.Fv, 82.80.Ms

The termination of well-defined silicon surfaces by hydrogen is an important problem because hydrogen atoms influence the structure, diffusion, and chemical reactivity at the surface. Dangling bonds, needed for chemical reactions and growth to proceed, may be generated by H-atom abstraction of terminating H atoms [1], or thermal desorption of H₂ [2]. The first process is considerably more complex than suggested by an ideal nonthermal Eley-Rideal mechanism [1]. For the thermal desorption process a nearly equivalent transition state involving one silicon atom was postulated for different surfaces such as the Si(100)-(2 × 1) and the Si(111)-(7 × 7) surface, despite a deviating kinetic behavior [3]. To understand these processes and the central role played by hydrogen atoms in the processing of Si-based materials, the elementary steps must be investigated in more detail such as the direct dissociation of the lattice-terminating SiH bond, creating H atoms and dangling bonds without strong heating, and the hopping of dangling bonds between adjacent sites if this process is faster than desorption of hydrogen [4].

Direct dissociation of the SiH bond of monohydride-terminated Si surfaces was achieved recently by electronic excitation with the low-energy electrons emitted from the scanning tunneling microscope (STM) tip [5]. This electron-stimulated desorption process was studied for the Si(111)-(1 × 1):H [5] and the Si(100)-(2 × 1):H surface [6] and had a threshold of 6–7 eV and a conversion efficiency of 10^{-6} – 10^{-8} . The STM method yields the corresponding structural effects at the surface; however, no direct information on the desorption products.

In this work we demonstrate for the first time the vacuum ultraviolet (VUV) laser-induced direct photochemical dissociation of SiH bonds on the Si(111)-(1 × 1):H surface. Results are reported for the 4 eV photons of a XeCl laser (308 nm), which initiate photothermal hydrogen desorption, and the 7.9 eV photons of a F₂ laser (157 nm), which induce photochemical desorption. The time-of-flight (TOF) analysis of the photodesorption products provides complementary information on the elemen-

tary bond-breaking process and the Si/H potential-energy surface (PES).

All desorption experiments were performed under ultrahigh vacuum (UHV) conditions (base pressure about 10^{-9} mbar) with the Si sample at room temperature. The chamber was equipped with a high-precision manipulator and load-lock system. TOF distributions were measured with a quadrupole mass analyzer (QMA) as demonstrated in [7]. The quadrupole filter was used in the perpendicular configuration to avoid detection of backscattered particles, and it was equipped with a differential pumping unit (liquid-N₂ cryo shield).

Figure 1 shows a sketch of the UHV system and the optical setup. A shutter allowed single-pulse measurements, while the laser was run with a fixed repetition rate for reasons of stability. The power of this pulse was measured by a fast photodiode and monitored by a digital storage oscilloscope. The second channel of the oscilloscope recorded the TOF distribution of the desorbed species.

The XeCl laser was operated with neon as buffer gas to obtain higher output with longer pulses (55 ns). The pulse duration had no influence on the TOF distributions as their typical widths were in the microseconds range (see top of Fig. 1). The F₂ laser pulse duration was 20 ns. Depending on the experiment, the photon flux was focused or weakened.

The silicon samples were prepared by wet chemical processing using a buffered HF solution to remove the oxide layer [8]. After the final rinsing in ultrapure water, the sample was purged with dry nitrogen gas and transferred to UHV immediately. Successfully prepared monohydride-terminated Si samples showed no water signal in the QMA spectra and no hydrocarbons remained on the surface. To test the surface quality, fragments of prepared samples were regularly analyzed by spectroscopic ellipsometry, to determine the microscopic roughness and void fraction [9], and by Fourier transform infrared (FTIR) spectroscopy, to measure the line profile of the terminating SiH bond [10].

To get an optimum signal-to-noise ratio, the samples were placed about five centimeters from the ion source of the mass analyzer. The TOF distributions were evaluated according to this distance and the drift time, which is a characteristic constant given by the atomic mass and the electric fields and voltages within the QMA [11]. The measured signal $S(t)$ could be fit by the Maxwellian distribution

$$S(t)dt \propto \frac{1}{(t - t_d)^2} \exp\left(-\frac{m}{2kT(t - t_d)^2}\right) dt, \quad (1)$$

where t_d denotes the drift time correction, m the mass of the desorbed particle, and T the absolute temperature. The unusual form of this expression is a consequence of the line focus used to obtain a stronger signal. Because of the additional dimension of the source, the propagation of the desorbing species is reduced in one direction.

To support the experimental results we simulated the desorption process. The surface temperature jump was

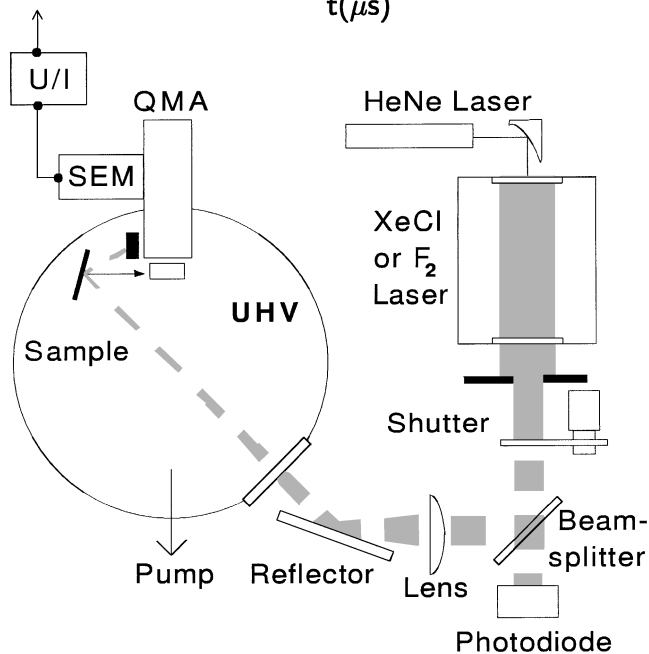
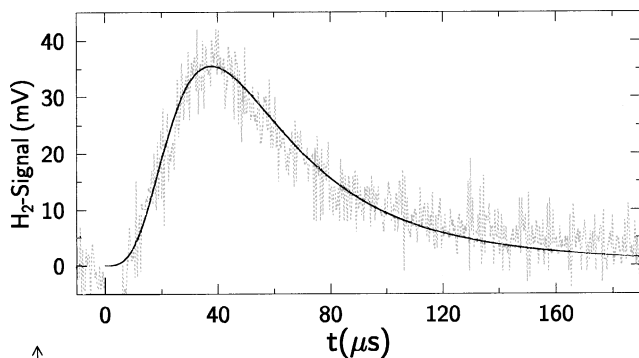


FIG. 1. The experimental setup showing the path of laser light and the perpendicular configuration of desorption flux and detection with the QMA. In the top graph a TOF signal is shown for the photochemical desorption with a F_2 laser and the corresponding Maxwellian fit (solid line).

calculated by solving the heat diffusion equation for silicon numerically by the method of finite differences. The constants for the simulation were taken from [12]. The calculations provided a heat distribution, which was used to determine the thermal desorption. In agreement with the Maxwellian distributions observed, we found that no Knudsen layer was formed [13], which would change the shape of the TOF distributions [7,14].

No hydrogen signal was observed for a photon flux of up to 50 mJ/cm^2 XeCl laser radiation. As soon as the laser-induced temperature jumped from room temperature significantly above the critical temperature of 800 K, thermal desorption of molecular hydrogen was observed. This was reached at fluences above 100 mJ/cm^2 . The yield increased exponentially with fluence, as can be seen in Fig. 2. This is typical for a thermally activated process.

The XeCl laser pulses heated the surface to high temperatures as reflected in Fig. 3. The error bars in the experimental results originate from the uncertainty in the TOF distributions. For hot species the distributions are narrower, leading to larger errors. The temperature calculations are also presented in Fig. 3, based on the fact that the TOF temperatures are related to the surface temperature. The simulations took into account that the desorption temperature is an integral over a spatial distribution with a transient time behavior, i.e., different from the maximum surface temperature. The bending of the simulated curve for fluences higher than 500 mJ/cm^2 reflects the beginning of local melting of silicon.

In the F_2 laser experiments desorption was observed even for very small fluences and the yield rose linearly

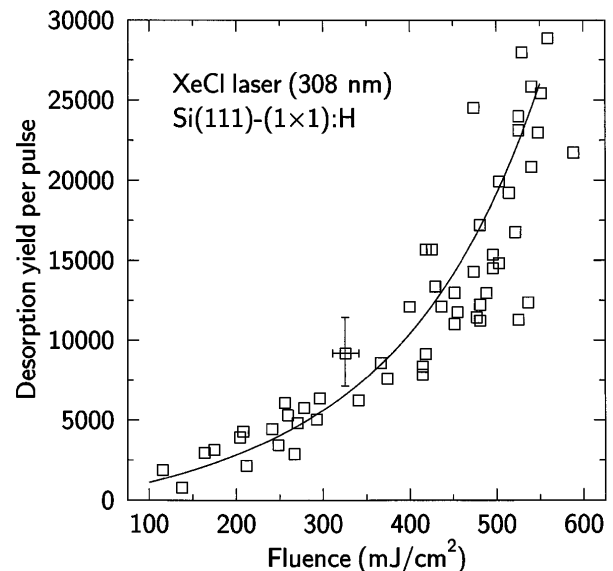


FIG. 2. Laser-induced thermal desorption with a XeCl laser. The desorption yield grows exponentially with fluence, as expected for a thermal mechanism. The solid line is a guide to the eye. The desorption yields are determined by integrating over the TOF distributions, and can be directly compared with the yields shown in Fig. 4.

with the number of 7.9 eV photons, demonstrating the direct bond-breaking process (see Fig. 4). The error bars are due to the base pressure, which mainly consisted of hydrogen. It contributed up to 90% of the signal and had to be subtracted to determine the desorption yield. Because of the transient nature of the signal and a constant background, the signal-to-noise ratio was nevertheless better than 3:1.

To minimize the thermal contribution to the electronic desorption process the F_2 laser fluence was limited to 5 mJ/cm^2 . The laser pulses caused a maximum temperature jump of 17 K, as indicated by the simulations, excluding a thermal desorption process. The TOF temperatures of the Maxwellian distributions are shown in Fig. 5 for varying photon fluxes. Their independence of the irradiation strength, within the error of about $\pm 100 \text{ K}$, indicates the photochemical character of the desorption process. The decrease of the desorption yield with the integrated photon flux was used to determine the cross section of photodesorption of H_2 , giving $(1.2 \pm 0.8) \times 10^{-20} \text{ cm}^2$.

Despite a careful analysis we were not able to detect unambiguously desorbed hydrogen atoms. One reason was due to the fact that atomic hydrogen is always formed from molecular hydrogen in the ion source by electron impact. The second was that because of the comparably short distance for propagation ($\sim 5 \text{ cm}$) the TOF distributions of the desorbed H and H_2 species could not be separated in time.

Up to now only hydrogen atoms have been considered as desorbing species for direct electronic desorption [5,6].

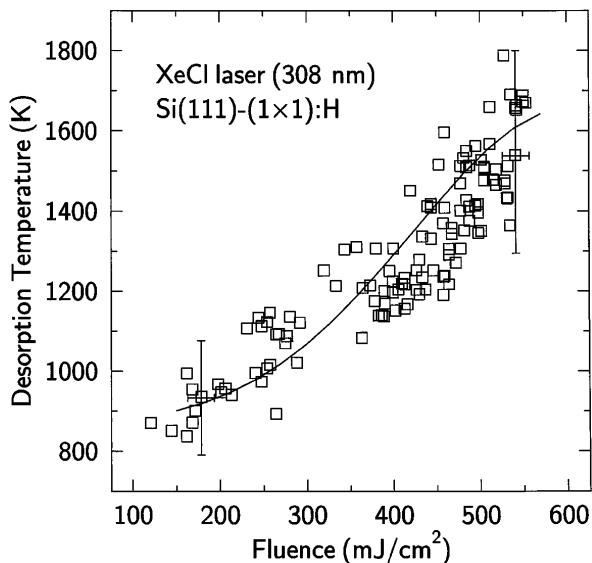


FIG. 3. Temperatures of desorbing hydrogen determined by a Maxwellian fit of the TOF distributions. A strong fluence dependence of the temperature could be observed for the irradiation of the surface with the focused XeCl laser beam. The solid line represents the simulation (finite-difference calculation) of the surface temperature.

To understand the origin of molecular hydrogen we modeled the microscopic desorption process by a molecular dynamics simulation using a Tersoff-type potential for Si-Si, Si-H, and H-H interaction [15]. It takes into account that the binding energies depend on the ambient configuration, i.e., on the distances and, in a minor way, on the angles to the surrounding atoms. The cluster representing the Si(111) surface consisted of 19 hydrogen and 73 silicon atoms. The molecular dynamics simulation exhibited the same characteristics as the frequently performed quantum dynamics calculations. The astonishing experimental feature that hydrogen desorbs translationally cold could neither be explained by our molecular dynamics method for Si(111)-(1 × 1):H nor by quantum dynamics calculations for Si(100)-(2 × 1):H [16,17].

The simulations considered the desorption of atomic hydrogen as the primary process. The kinetic energies of the desorbing atoms were estimated from the potential energy curves and lifetime using a theory developed for electron-stimulated desorption [18]. The first step is the electronic excitation of the Si-H bonding σ orbital to an unoccupied antibonding σ^* orbital. Because of the repulsive character of the excited state, the hydrogen atom gains kinetic energy. To explain the H/D isotope effect, very high quenching rates of $3 \times 10^{15} \text{ s}^{-1}$ have been assumed for the repulsive excited state [18]. According to this mechanism dissociation competes with quenching on the time scale of bond cleavage, and therefore the desorption occurs predominantly from the highly excited electronic ground state.

For the VUV-photon process we assume this scenario as the basis for the molecular dynamics simulation. Accepting the quenching rate mentioned above the hydrogen

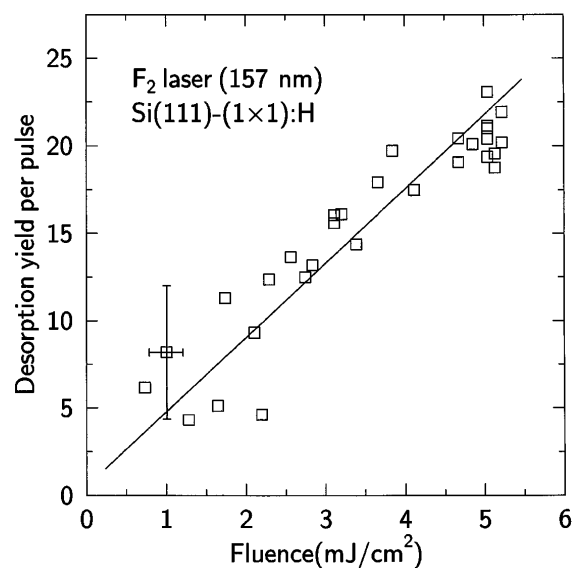


FIG. 4. The linear rise of the desorption yield with fluence demonstrates the photochemical character of the VUV-photon (157 nm) process. The yield values can be directly compared with those of Fig. 2.

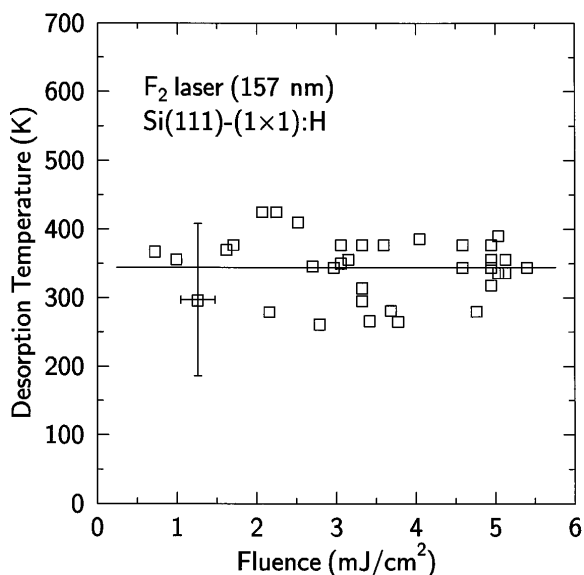


FIG. 5. The desorption temperature is found to be independent of fluence in the case of desorption induced by the F_2 laser photons (7.9 eV). The fit gave a constant desorption temperature of 350 K close to room temperature. Note that the expected increase of 17 K is within the experimental error of ± 100 K.

atoms desorb with a kinetic energy of about 0.1 eV. For atoms having flight directions deviating strongly from the surface normal, the simulations show that desorption of molecular hydrogen becomes possible. The formation of H_2 follows from the interaction of the photochemically desorbed hydrogen atoms with a neighboring surface H atom and the strong H_2 binding energy. The simulation yielded, as a rough estimate, a total fraction of 10%–20% for the formation of molecular hydrogen, and therefore could explain the experimentally observed desorption of H_2 . An atomic and molecular hydrogen desorption channel has been seen before in synchrotron-desorption experiments covering a large range from 10–1000 eV [19].

The molecular path observed here has an efficiency of $\sim 7 \times 10^{-6}$. Therefore, the whole photon-stimulated process probably has a distinct higher yield than bond breaking by electrons. Also, the threshold energies may be different for the electron and photon-stimulated process. For electron bombardment a threshold of about 6.5 eV was found, corresponding to the excitation of electrons with nonzero parallel wave vector, while for vertical optical transitions a value of 8.5 eV has been calculated [5]. We found 4.0 eV to be below the threshold energy, while 7.9 eV photon energy is enough for electronic excitation and desorption. To determine the exact threshold for the photon process, additional experiments are needed.

In summary, we have shown that direct breaking of surface bonds is possible with VUV photons. This process of dangling-bond formation occurs at room temperature, is contact free, and allows an efficient manipulation of surface chemistry and processing. Photolytic dissociation of surface-terminating species is of interest for technological applications such as photon-induced etching, growth, and catalysis. Photochemical processing has the advantages that it can be performed with low laser pulse energy, which means minimal temperature increase, and high spatial resolution without the risk of destroying, e.g., doping profiles.

Financial support of the equipment used in this work by the Deutsche Forschungsgemeinschaft (DFG), the Bundesministerium für Bildung und Forschung (BMBF), and the Fonds der Chemischen Industrie is gratefully acknowledged.

- [1] S. A. Buntin, *J. Chem. Phys.* **108**, 1601 (1998).
- [2] K. W. Kolasinski, W. Nessler, A. de Meijere, and E. Hasselbrink, *Phys. Rev. Lett.* **72**, 1356 (1994).
- [3] S. F. Shane, K. W. Kolasinski, and R. N. Zare, *J. Chem. Phys.* **97**, 1520 (1992).
- [4] M. McEllistrem, M. Allgeier, and J. J. Boland, *Science* **279**, 545 (1998).
- [5] R. S. Becker, G. S. Higashi, Y. J. Chabal, and A. J. Becker, *Phys. Rev. Lett.* **65**, 1917 (1990).
- [6] T.-C. Shen, C. Wang, G. C. Abeln, J. R. Tucker, J. W. Lyding, Ph. Avouris, and R. E. Walkup, *Science* **268**, 1590 (1995).
- [7] R. Braun and P. Hess, *J. Chem. Phys.* **99**, 8330 (1993).
- [8] P. Dumas, Y. J. Chabal, and P. Jakob, *Surf. Sci.* **269/270**, 867 (1992).
- [9] M. Barth and P. Hess, *Appl. Phys. Lett.* **69**, 1740 (1996).
- [10] J. Knobloch and P. Hess, *Appl. Phys. Lett.* **69**, 4041 (1996).
- [11] R. Braun and P. Hess, *Int. J. Mass. Spectrom. Ion Process.* **125**, 229 (1993).
- [12] G. G. Bentini, M. Bianconi, and C. Summonte, *Appl. Phys. A* **45**, 317 (1988).
- [13] R. Kelly, *J. Chem. Phys.* **92**, 5047 (1990).
- [14] L. V. Zhigilei and B. J. Garrison, *Appl. Phys. Lett.* **71**, 551 (1997).
- [15] M. V. Murty and H. A. Atwater, *Phys. Rev. B* **51**, 4889 (1995).
- [16] A. C. Luntz and P. Kratzer, *J. Chem. Phys.* **104**, 3075 (1996).
- [17] M. R. Radeke and E. A. Carter, *Annu. Rev. Phys. Chem.* **48**, 243 (1997).
- [18] Ph. Avouris, R. E. Walkup, A. R. Rossi, T.-C. Shen, G. C. Abeln, J. R. Tucker, and J. W. Lyding, *Chem. Phys. Lett.* **257**, 148 (1996).
- [19] H. Akazawa and Y. Utsumi, *J. Appl. Phys.* **78**, 2725 (1995).